

On the loss of coherence in double-slit diffraction of neutrons

R. Tumulka,^{1,*} A. Viale,^{2,†} and N. Zanghì^{2,‡}

¹*Mathematisches Institut, Eberhard-Karls-Universität,
Auf der Morgenstelle 10, 72076 Tübingen, Germany*

²*Dipartimento di Fisica, Istituto Nazionale di Fisica Nucleare,
Sezione di Genova, Via Dodecaneso 33, 16146 Genova, Italy*

(Dated: 9th February 2020)

In diffraction experiments with particle beams, several effects lead to a fringe visibility reduction of the interference pattern. We theoretically describe the intensity one can measure in a double-slit setup and compare the results with the experimental data obtained with cold neutrons. Our conclusion is that for cold neutrons the fringe visibility reduction is due not to decoherence, but to initial incoherence.

PACS numbers: 03.65.Yz, 03.65.Ta, 03.75.Dg

I. INTRODUCTION

We provide a theoretical description of the intensity pattern in double-slit experiments with neutrons, with specific attention to the *cold* neutron diffraction ($\lambda \approx 20 \text{ \AA}$) carried out by Zeilinger *et al.* in 1988 [1].

Usually, the main problem in the analysis of diffraction experiments is to establish exactly which causes bring about the loss of coherence experimentally inferred from the detected signal. In fact, it is well known that a certain loss of coherence in interfering beams is responsible for a fringe visibility reduction and that it can be produced both by the initial preparation of the beam (namely, the non-dynamical *incoherence*) and by the interaction of its constituting particles with the environment (namely, the dynamical *decoherence*) [2, 3, 4, 5, 6, 7, 8, 9, 10, 11]. Only a detailed description of the intensity pattern or specific tests conducted in the laboratory allow to quantify the weight of each single cause.

We develop our analysis in the theoretical framework reported in Ref. [8], but provide new calculations and numerical simulations in order to deal with an incoherence cause not considered in Ref. [8], which we propose plays a role in explaining the experimental data of Ref. [1]. This cause is that the width of the wave function impinging on the double-slit is comparable with the spatial scale defined by the double-slit setup (i.e., the distance between the two slits and the slit apertures). We argue, using a numerical solution of the Schrödinger equation, that this feature of the incoming wave function leads to a slight difference in transverse momentum between the two wave packets emanating from the grating, such that the centers of the packets move apart. This momentum difference was already suggested in Ref. [11], but no physical explanation was given. It proves relevant for fitting the data of Ref. [1].

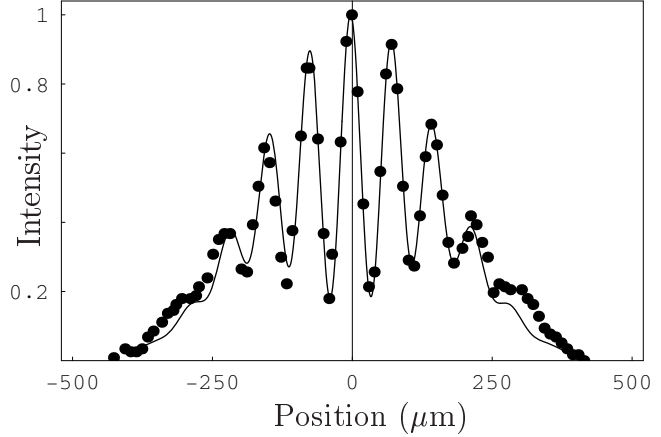


Figure 1: Comparison between theoretical prediction derived here (solid line) and experimental data taken from [1] (circle point) for neutron double-slit diffraction.

We determine the degree of coherence for such a neutron beam, under the conditions of a typical interferometer, and a detailed prediction of the intensity pattern. The result we obtain is shown in Fig. 1. We find that in the experiment of Ref. [1] decoherence does not play any role in the fringe visibility reduction, which indeed is entirely due to incoherence of the source. This conclusion is opposite to that of Ref. [11], where it is claimed that decoherence is essential for explaining the data from [1]. We comment on this claim in the end of Sec. II B below.

II. VISIBILITY REDUCTION IN THE INTENSITY PATTERN

In interferometry experiments, several losses of coherence affect a particle beam, due both to its preparation and its evolution, with the consequence of a fringe visibility reduction of the detected intensity pattern. In detail, the causes of *incoherence* are mainly the angular

*Electronic address: tumulka@everest.mathematik.uni-tuebingen.de

†Electronic address: viale@ge.infn.it

‡Electronic address: zanghi@ge.infn.it

divergence and the non-monochromaticity of the beam, while *decoherence* channels can be collisions with environmental particles, interaction with the grating and, for atoms and structured molecules, photon emissions. Clearly, these effects correspond either to randomness of the wave function of the system, due to the experimental difficulty in the production of the same initial state for all the particles (leading to a *statistical mixture*), or to entanglement of the system with the surrounding environment. Therefore, in order to obtain the *local intensity* revealed on a *distant* screen, we have to evaluate in such conditions the statistical reduced density matrix. In fact, the intensity is proportional to the diagonal elements of the density matrix, evaluated at the *time of arrival* $T = L/v$, where L is the distance between the screen and the grating, and v the particle velocity (for more details see Refs. [8, 12]).

In the following we shall describe the various coherence losses which can occur within neutron interferometry.

A. Initial incoherence

In the initial preparation of a beam, it is problematic to keep a perfect control on the *monochromaticity* and on the *collimation* of the beam, i.e., it is quite impossible to supply the same velocity with the same direction to all the beam particles and still obtain an appreciable signal on the detection screen.

First of all, we consider the non-monochromaticity, since every spectral component of the beam contributes incoherently to each other. In our case, assuming that the detection screen is placed orthogonally to the y direction (the direction of propagation of the beam) and that the grating is translation invariant in the z direction (see Fig. 2), the intensity observed on the screen at coordinate x is

$$I(x) = \int d\lambda f(\lambda) I_\lambda(x), \quad (1)$$

where $f(\lambda)d\lambda$ is the wavelength distribution of the beam and $I_\lambda(x)$ the intensity corresponding to a single wavelength λ . Thus, one can continue the analysis with a single wavelength and postpone the integration (1) to the final step (see Sec. IV).

Concerning the collimation of the beam, we assume that the particle source emits *random wave functions*, whose randomness lies in the deviation of its direction of propagation from the y direction, corresponding to imperfect collimation. Since we are interested in interference only in the x -direction, we consider just the x -component k_x of the random wave vector thus produced. Therefore, we write the *incoming* wave function ψ_{in} at the diffraction grating as

$$\psi_{\text{in}}(\mathbf{r}; k_x) = \varphi_0 \left[\mathbf{r} - f k_x \mathbf{e}_x \right] e^{i k_x x} \text{ with } f \equiv \frac{\lambda(L_1 + L_2)}{2\pi},$$

where $\varphi_0(\mathbf{r})$, $\mathbf{r} = (x, y, z)$, is the wave function produced by the source in case of perfect collimation, λ the neutron

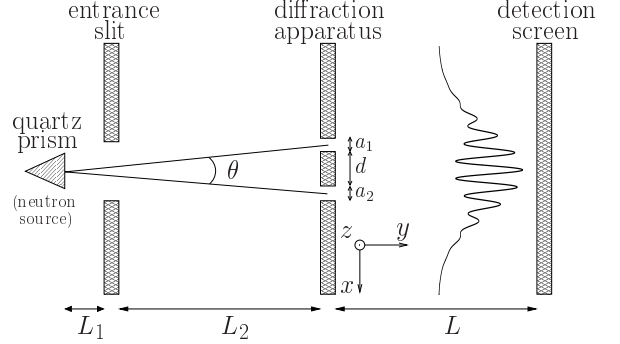


Figure 2: Sketch of the geometry of a collimation setup as in [1] (not to scale).

wave length, $L_1 + L_2$ the distance from the source to the grating (see Fig. 2) and \mathbf{e}_x the unit vector of the x -axis. The shift $k_x f$ along the x -direction is kinematically obtained by evolving a neutron, with a x -velocity $\hbar k_x/m$, for the time necessary to cover the distance $L_1 + L_2$ with the y -velocity $\hbar/(m\lambda)$. Note that we have neglected the spread of the wave function during the travel, since it is irrelevant for our analysis. Note also that the presence of this shift is somehow a consequence of the finite width of the neutron wave function compared to the scale fixed by the grating dimensions. Indeed, if the width of the wave function support is very large, this shift can be neglected, as in the usual analysis of the initial state preparation in matter wave interferometry (see Ref. [8] and references therein).

The wave function after the passage through the double-slit (the *outgoing* wave function) can be expressed as a superposition of two packets $\varphi_1(\mathbf{r})$ and $\varphi_2(\mathbf{r})$ emanating from the left respectively right slit, with weights c_1 and c_2 according to

$$\psi_{\text{out}}(\mathbf{r}; k_x) = [c_1 \varphi_1(\mathbf{r}) + c_2 \varphi_2(\mathbf{r})] e^{i k_x x} \quad (2)$$

with $\|\varphi_1\| = \|\varphi_2\| = 1$. We estimate the coefficients as

$$c_i = c_i(k_x) = \varphi_0(\mathbf{r}_i - f k_x \mathbf{e}_x)$$

with \mathbf{r}_i the position of the center of slit i . Thus the wave packet emanating from slit 1 has greater weight $|c_1|^2$ if the incoming wave packet is closer to slit 1. (For further discussion see Ref. [20].)

Assuming that φ_0 is a Gaussian wave packet—with mean 0 and standard deviation s —and assuming a Gaussian probability distribution for the wave number k_x —with mean 0 and standard deviation σ_{k_x} —the resulting mixture of the wave functions (2) yields the state

$$\rho_{\text{out}}(\mathbf{r}, \mathbf{r}') = \rho_{11}(\mathbf{r}, \mathbf{r}') + \rho_{12}(\mathbf{r}, \mathbf{r}') + \rho_{21}(\mathbf{r}, \mathbf{r}') + \rho_{22}(\mathbf{r}, \mathbf{r}'), \quad (3)$$

where, for $i, j = 1, 2$,

$$\rho_{ij}(\mathbf{r}, \mathbf{r}') \equiv \frac{s\mathcal{N}}{\sqrt{s^2 + 2f^2\sigma_{k_x}^2}} \exp\left[-\frac{(x_i^2 + x_j^2)}{2s^2}\right] \varphi_i(\mathbf{r}) \varphi_j^*(\mathbf{r}') \exp\left\{\frac{\sigma_{k_x}^2 s^2}{2(s^2 + 2f^2\sigma_{k_x}^2)} \left[\frac{f}{s^2}(x_i + x_j) + i(x - x')\right]^2\right\}, \quad (4)$$

with \mathcal{N} a normalization constant.

B. Decoherence

In the treatment of decoherence, we make explicit use of the fact that we are concerned with neutrons, in particular at the low energies of Ref. [1]. In this case, in fact, the only relevant decoherence channel—if any—consists in collisions with air molecules, so that the dynamics can be modelled within a Markovian description of the scattering event, in particular in the *large scale* approximation allowed by air molecules (see [2, 8, 13]). The model obtained in this way allows an estimate of the neutron *coherence time* τ_{coh} [8, 13]:

$$\tau_{\text{coh}} = \frac{1}{P(\Theta_{\mathcal{E}}) \sigma_{\text{tot}}} \sqrt{\frac{8}{\pi k_B \Theta_{\mathcal{E}} m_{\text{air}}}}, \quad (5)$$

where $P(\Theta_{\mathcal{E}})$ is the environmental pressure at the temperature $\Theta_{\mathcal{E}}$, σ_{tot} the total cross section of the scattering events, k_B the Boltzmann constant and $m_{\text{air}} \approx 4.8 \cdot 10^{-26}$ Kg the mean mass of air molecules. (Eq. (5) takes into account a correction by a factor 2π , usually missing in the literature, that was theoretically predicted in [14, 15] and experimentally checked in [9].)

The result is that τ_{coh} is much greater than the time of flight, even in extreme experimental situations. In fact, even considering a surrounding pressure of 1 atm (though typically “the beam paths along the optical bench” are “evacuated in order to minimize absorption and scattering” [1]) and room temperature, for an estimated total cross section of 10^{-27} m^2 [21] we obtain that

$$\tau_{\text{coh}} \approx 140 \text{ s}. \quad (6)$$

This time—not much smaller than the neutron lifetime—shows that the coherence is fully kept for the duration of most experiments. For instance, in [1] the mean time of flight is $T \approx 0.023$ s, several orders of magnitude smaller than τ_{coh} .

For this reason, in the following we shall consider the neutron beam uncoupled from its environment and shall describe the dynamics through the usual unitary Schrödinger evolution.

This conclusion contradicts that of Sanz *et al.* in Ref. [11], who claim that “decoherence is likely to exist in Zeilinger *et al.*’s experiment.” Indeed, their own calculations do not support their conclusion. The basis of their claim is that the *damping term* Λ_t in their expression for the observed intensity pattern [see their Eq. (27)] turns

out, when fitted to the data, to be nonzero. However, this term could just as well represent *incoherence* instead of decoherence (as does for example the similar quantity \mathcal{A} in their Eq. (16), or the *coherence length* in Eq. (47) of Ref. [8]) [22]. Indeed, our estimate (6) of the coherence time shows that the damping Λ_t cannot be attributed to decoherence.

III. PASSAGE THROUGH THE GRATING

A. General features

Before establishing how we can describe the intensity pattern produced by neutrons which leave the grating in the state (3)–(4) and evolve freely toward the detection screen, we want to give a more detailed analysis of the diffraction through the double-slit, in order to characterize better the packets φ_1 and φ_2 split by the grating.

In general, the passage through the grating can produce vibrations or other kinds of interaction with the walls of the grating—as the van der Waals forces in case of atomic and molecular beams [17]—able to corrupt the visibility of the interference pattern. Moreover, also the finite size of the grating and differences in the slit apertures can yield the same result, especially in case of complex molecules [9, 18].

For our purpose, since cold neutrons do not interact much with matter and, in this kind of problem, can be treated as elementary particles, all these effects can be neglected. Nevertheless, another important feature emerges from the analysis of the diffraction in the conditions we are investigating. In fact, the outgoing packets φ_1 and φ_2 turn out to possess two slightly divergent momenta p_1 and p_2 in the transverse x —direction, causing a *relative drift* that progressively increases the distance between the centers of the two packets. Even though this behavior does not reduce the fringe visibility, it can significantly affect the shape of the interference pattern, changing the overlap of the two packets and so the position of secondary minima and maxima.

This effect can be predicted by numerically solving the Schrödinger equation for the passage of the neutron wave function through the grating.

B. Numerical simulations

Without loss of generality, we consider a *monochromatic* particle with velocity *perfectly perpendicular* to the

grating extension, since any deviation from these assumptions is independently taken into account by means of the integration (1) and of the statistical mixture which leads to the state (3)–(4). Under these simplifications, the only unknown parameter entering the numerical simulation is the spatial extension s of the wave function before the grating.

We have treated the problem as bidimensional in the xy –plane. We have discretized the physical space into a grid of $N_x N_y$ points, spaced by Δx in the x –direction and Δy in the y –direction. The diffraction grating is modelled as an impenetrable barrier, i.e., a barrier with height equal to several times the mean kinetic energy of the neutrons. The size and shape of the grating in the simulation we describe later. The potential barrier and the wave function before the grating have been discretized on the grid and the latter has been evolved using the *leapfrog method* [19].

Due to the specific characteristics of the physics we are trying to simulate, we have encountered a serious difficulty with the numerical treatment. In order to evolve a given wave function, it is necessary to perform a spatial discretization with mesh width at most of the order of λ , the wave length of the wave function. If this condition is not respected, the numerical solution cannot be expected to be close to the exact one, and may describe a completely different dynamics (for examples and more details see Ref. [20] and references therein). Our problem consists in the fact that the spatial scale we can afford is much greater than λ : As depicted in Fig. 6 of Ref. [1], the double-slit alone extends in the y –direction over the tenth of a millimeter, and the entire diffraction apparatus, with the shape of two wedges pointing to each other with the double-slit between their tips, has a size of ten millimeters. Therefore, the necessary number of grid points would be, for each dimension, at least $0.1 \text{ mm}/\lambda \approx 50,000$ or even $10 \text{ mm}/\lambda \approx 5,000,000$. The problem is that so many points per dimension are too much for the memory capabilities of a typical workstation.

In the light of these considerations, we prefer to supply just a qualitative explanation of the phenomenon, making some drastic simplifications. First of all, we schematize the complex shape of the grating used in Ref. [1] as a rectangular double-slit, with apertures a_1 and a_2 and distance d between the apertures as reported in Ref. [1], but with thickness very smaller than the real value. Then we perform the numerical simulations in correspondence of a set of Δx and Δy greater than λ , asymptotically fulfilling an extrapolation of the limit for Δx and $\Delta y \rightarrow \lambda$ from this series of values. We remark that, even if this limit procedure were not accurate, our purpose is only to show the presence and the characteristics of the mechanism which produces the two momenta, whose specific values in the theoretical formulation of the intensity pattern of Ref. [1] have to be fitted.

The main result we obtain is that the two momenta are really produced in opposite directions, outgoing from the double-slit setup, and that their values, in modulus,

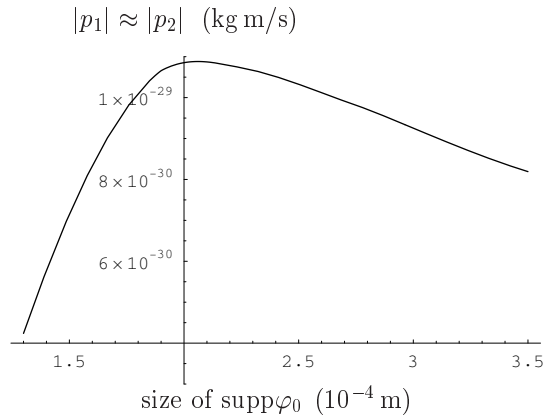


Figure 3: Transverse momenta p_1 and p_2 as function of the size of the support of the wave function before the grating. Here the value of b , the thickness of the grating, was taken equal to 10^{-7} m .

are practically the same (a difference of about (2–3)% is due to a slight asymmetry of $a_1 = 21.9 \mu\text{m}$ and $a_2 = 22.5 \mu\text{m}$).

In Fig. 3 it is reported the behavior of the production of such transverse momenta p_1 and p_2 for varying the wave function support, in correspondence of the value $b = 10^{-7} \text{ m}$, for computational facilitation. Note that for $s = \text{supp } \varphi_0 \lesssim d \approx 10^{-4} \text{ m}$ the wave packet is quite totally reflected, so that p_1 and p_2 are substantially zero. Moreover, it results that p_1 and p_2 tends to zero in the limit $s \rightarrow \infty$ in which $\varphi_0(\mathbf{r})$ becomes a plane wave.

IV. DETECTION OF THE INTENSITY PATTERN

As motivated in the previous section, the propagation of the density matrix from the double-slits toward the screen is given by the free Schrödinger evolution. Since we can assume classical motion in the propagation direction y and have already mentioned the translational invariance of the grating in the z –direction, the relevant quantum mechanical analysis is one-dimensional along the x –direction. Thus, we obtain the evolution

$$\rho_t(x, x') = \iint dy dy' K(x, t; y, 0) K^*(x', t; y', 0) \rho_{\text{out}}(y, y'), \quad (7)$$

where

$$K(x, t; y, 0) = \sqrt{\frac{m}{2\pi\hbar t}} \exp \left[\frac{im}{2\hbar t} (x - y)^2 \right],$$

with m the mass of the beam particle, and where $\rho_0(y, y')$ is given by Eqs. (3) and (4) written in case of one dimension. Moreover, as already stated and well motivated in the literature [8, 12], the intensity pattern measured on a screen is proportional to the diagonal elements of the density matrix evaluated at $T = mL\lambda/(2\pi\hbar)$, the time of

arrival on the screen:

$$I_\lambda(x) \sim \rho_T(x, x). \quad (8)$$

For the analytical computation of $I_\lambda(x)$, we suppose that the outgoing packets φ_1 and φ_2 have Gaussian shape, with transverse momenta p_1 and p_2 acquired during the passage through the double-slit, as motivated in previous section. An analytic expression for $\rho_T(x, x)$ can be obtained as is reported in Ref. [20] but is of no particular interest here.

In the purpose of compare our theoretical results with measured data, we have finally to consider the finite spatial resolution x_0 of the detector. For example, in case of *flat response* on the interval $[x - \frac{x_0}{2}, x + \frac{x_0}{2}]$ around each position x , the intensity is given by

$$I(x) = \frac{1}{x_0} \int_{x - \frac{x_0}{2}}^{x + \frac{x_0}{2}} dy I_\lambda(y),$$

or better, taking into account the wavelength spread (1) previously left out, by

$$I(x) = \frac{1}{x_0} \int d\lambda f(\lambda) \int_{x - \frac{x_0}{2}}^{x + \frac{x_0}{2}} dy I_\lambda(y). \quad (9)$$

In this regard, note that numerical simulations show that, in the above integration, p_1 and p_2 can be considered constant, since their values are substantially the same for λ which varies within the range of wave lengths selected for the experiment. Finally, note that both x_0 and $f(\lambda)$ are directly deduced from Ref. [1].

In Fig. 1 we have reported the result of our theoretical prediction. We have considered Gaussian shapes for the two outgoing packets φ_1 and φ_2 [which enter in the expression (8) of the intensity via Eqs. (7) and (9)], with standard deviations σ_1 and σ_2 adapted to the extensions a_1 and a_2 of the slits. More precisely, we have chosen σ_i equal to the standard deviation of a *uniform* probability distribution over an interval of length a_i , i.e., $\sigma_i = a_i/\sqrt{12}$, $i = 1, 2$. The following parameters were obtained by a *fit procedure*: the support size $s = 40 \mu\text{m}$, the two momenta $p_1/m = -0.0034 \text{ m/s}$ and $p_2/m = 0.0029 \text{ m/s}$ [23], and the angular divergence of the beam $\sigma_{k_x} = 4976 \text{ m}^{-1}$. Moreover, a constant background has been subtracted from experimental data.

[1] A. Zeilinger, R. Gähler, C. G. Shull, W. Treimer, and W. Mampe, Rev. Mod. Phys. **60**, 1067 (1988).

[2] E. Joos, H. D. Zeh, C. Kiefer, D. Giulini, J. Kupsch, and I.-O. Stamatescu, *Decoherence and the Appearance of a Classical World in Quantum Theory*, Second Edition, Springer, Berlin (2003).

[3] T. Pfau, S. Spälter, Ch. Kurtsiefer, C. R. Ekstrom, and J. Mlynek, Phys. Rev. Lett. **73**, 1223 (1994).

[4] H. M. Wiseman, Phys. Rev. A **56**, 2068 (1997).

[5] T. P. Altenmüller, R. Müller, and A. Schenzle, Phys. Rev. A **56**, 2959 (1997).

[6] R. Alicki, Phys. Rev. A **65**, 034104 (2002).

[7] P. Facchi, A. Mariano, S. Pascazio, Recent Res. Dev. Phys. **3**, 1 (2002); quant-ph/0105110.

[8] A. Viale, M. Vicari, and N. Zanghì, Phys. Rev. A **68**, 063610 (2003).

[9] K. Hornberger, J. E. Sipe, and M. Arndt, Phys. Rev. A **70**, 053608 (2004).

[10] K. Hornberger, L. Hackermüller, and M. Arndt, Phys. Rev. A **71**, 023601 (2005); K. Hornberger, Phys. Rev. A **73**, 052102 (2006).

[11] A. S. Sanz, F. Borondo, and M. J. Bastiaans, Phys. Rev. A **71**, 042103 (2005).

[12] M. Daumer, D. Dürr, S. Goldstein, and N. Zanghì, J. Stat. Phys. **88**, 967 (1997).

[13] M. R. Gallis and G. N. Fleming, Phys. Rev. A **42**, 38 (1990).

[14] K. Hornberger and J. E. Sipe, Phys. Rev. A **68**, 012105 (2003).

[15] B. Vacchini, J. Mod. Opt. **51**, 1025 (2004).

[16] H. Palevsky and R. M. Eisberg, Phys. Rev. **98**, 492 (1955); T. J. Krieger and M. S. Nelkin, Phys. Rev. **106**, 290 (1957); J. A. Young and J. U. Koppel, Phys. Rev. **135**, 603 (1964).

[17] R. E. Grisenti, W. Schöllkopf, J. P. Toennies, G. C. Hegerfeldt, and T. Köhler, Phys. Rev. Lett. **83**, 1755 (1999).

[18] M. Božić, D. Arsenović, and L. Vušković, Phys. Rev. A **69**, 053618 (2004).

[19] A. Askar e A. S. Cakmak, J. Chem. Phys. **68**, 2794-2798 (1977).

[20] A. Viale, *Loss of coherence in matter wave interferometry*, Ph.D. dissertation, Department of Physics, University of Genoa, Italy (2006).

[21] To our knowledge, direct values of σ_{tot} in the considered conditions and with the molecules which compose the air (i.e., mainly nitrogen, but also oxygen and some trace of hydrogen) are not reported in literature. Nevertheless, starting from related measurements [16] and considering typical trends of the cross section, it is possible to estimate very roughly the bound $\sigma_{\text{tot}} \lesssim 10^{-27} \text{ m}^2$. However, even if a correct estimation of σ_{tot} would lead to a greater value, τ_{coh} would still be much larger than the time of flight T since five orders of magnitude lie between our estimate for τ_{coh} and T . Furthermore, we have assumed very unfavorable experimental circumstances.

[22] In particular, the caption of their Fig. 2 is incorrect in so far as Fig. 2(a) does not include incoherence, and Fig. 2(b) may represent either incoherence or decoherence.

[23] These values of p_1 and p_2 agree qualitatively with the estimates in Ref. [11]. Nonetheless, their estimation is dubious, as it is based on an incomprehensible application of the Heisenberg uncertainty principle.